Geophys. J. Int. (2003) **155,** 532–538

Implementing spectral leakage corrections in global surface wave tomography

Jesper Spetzler[1] and Jeannot Trampert[2]

[1] *Department of Applied Earth Sciences, TU Delft,* PO Box 5028, NL-2600 *GA Delft, the Netherlands. E-mail: j.spetzler@citg.tudelft.nl*
[2] *Faculty of Earth Sciences, Utrecht University,* PO Box 80021, NL-3508 *TA Utrecht, the Netherlands*

Accepted 2003 June 27. Received 2003 June 2; in original form 2002 July 14

SUMMARY

We analyse the effect of uneven ray coverage in global surface wave tomography. An inhomogeneous distribution of seismic rays may bias tomographic models because certain areas are better sampled than others. It is possible to suppress this bias, known as the spectral leakage, by using a linear inversion technique with a specific data weighting. We use finite-frequency sensitivity kernels to calculate the appropriate data weightings which suppress spectral leakage. Exact calculations are very computer intensive and approximations are needed. We give a rule-of-thumb for the parameters entering the approximation. We show that a low-degree phase velocity model constructed from real data, without special precaution, suffers from noticeable spectral leakage. This leakage effect is stronger than any contamination of the solution by data errors. Model damping cannot correct for spectral leakage unless the inverse problem is overparametrized. Model damping implies varying resolution of retrieved features and makes a precise geodynamic interpretation of the images difficult. Increasing computer power makes spectral leakage corrections possible, allowing tomographic images with perfect resolution.

Key words: finite-frequency effects, inverse problem, spectral leakage, surface wave tomography.

1 INTRODUCTION

Precise geodynamic understanding requires tomographic models of higher and higher precision. As a result of automatic data processing, surface wave tomography has made a great leap forward in recent years and the trend is to recover smaller and smaller scale structure by increasing the data coverage manifold and thus being able to reduce damping in the inversion. The risk is to push existing techniques beyond theoretical limitations. The limits of commonly used ray theory have been given by Wang & Dahlen (1995), who showed that the width of the first Fresnel zone has to be smaller than the scalelength of heterogeneity. Spetzler *et al.* (2002) analysed the biases introduced by ignoring this limitation. By reducing the damping, biases due to spectral leakage might become an issue (Trampert & Snieder 1996). It is common practice to truncate model expansions at a certain arbitrary spherical harmonic degree. Information in the data on the neglected basis functions may lead to spectral leakage due to uneven data coverage (Snieder *et al.* 1991). Spectral leakage is the mapping of small-scale structure not accounted for in the model expansion into the inverted low-degree structure.

We will investigate spectral leakage in a global surface wave tomographic experiment using the extensive phase velocity measurements of Trampert & Woodhouse (2001). Instead of using the great circle approximation, we implement finite-frequency data kernels calculated by Spetzler *et al.* (2002). We make spectral leakage corrections following Trampert & Snieder (1996) and compare the results to classical least-squares inversions (Tarantola 1987). The two inversions differ in the way that data are weighted. Trampert & Snieder (1996) used a synthetic modelling experiment without data errors. In our work, we specifically explore the effect of data errors on the solution using a spectral leakage inversion and a classical least-squares approach. As soon as the data weighting is changed in the inversion, data errors effect the final model differently. Classical least-squares inversions optimize noise propagation (Menke 1989), but spectral leakage corrections could change this.

In Section 2, we briefly review the theory for spectral leakage corrections. We explain, in Section 3, how the spectral leakage solution is combined with finite-frequency kernels from surface wave scattering theory. An extensive synthetic modelling experiment representative for global surface wave tomography is set up in Section 4. We focus on two main questions: what is a reasonable range for the parameters needed in a spectral leakage inversion and how strong is the influence of data error propagation using a realistic description of noise in our data set. In Section 5 we point out the differences in tomographic models, based on real data, obtained using spectral leakage corrections and the classical least-squares approach. A brief discussion follows in Section 6.

2 THEORY

A detailed description of spectral leakage and how to suppress it may be found in Trampert & Snieder (1996) and Snieder & Trampert

(1999, and http://samizdat.mines.edu). A continuous model parameter $m(x)$ at a point x may be expanded using a complete set of basis functions $B_j(x)$ with appropriate coefficients m_j. Such an expansion is generally infinite and can be decomposed into a part $m_L(x)$ up to an arbitrary truncation level L and a part $m_\infty(x)$, which is built from the remaining set of basis functions:

$$m(x) = \sum_{j=1}^{\infty} m_j B_j(x) = m_L(x) + m_\infty(x), \tag{1}$$

with

$$m_L(x) = \sum_{j=1}^{L} m_j B_j(x) \quad \text{and} \quad m_\infty(x) = \sum_{j=L+1}^{\infty} m_j B_j(x). \tag{2}$$

In linear theory, a datum d_i is found from

$$d_i = \int G_i(x) m(x)\, dx + e_i, \tag{3}$$

where $G_i(x)$ is the continuous data kernel and e_i is the error in d_i. Expressing $m(x)$ by its complete expansion of eq. (1) yields

$$d_i = \sum_{j=1}^{\infty} A_{ij} m_j + e_i, \tag{4}$$

where the forward matrix elements

$$A_{ij} = \int G_i(x) B_j(x)\, dx, \tag{5}$$

are the projection of the data kernel $G_i(x)$ on the basis functions $B_j(x)$. The discrete forward problem of eq. (4) may then be written in vector form as

$$\mathbf{d} = \mathbf{A}\mathbf{m} + \mathbf{e}. \tag{6}$$

Using the truncation level L, the least-squares solution of eq. (6) is

$$\tilde{\mathbf{m}}_L = \mathbf{A}_L^{-g}\mathbf{d}, \tag{7}$$

where $\mathbf{A}_L^{-g}$ is the inverse of the matrix $\mathbf{A}_L$ in the least-squares sense given by

$$\mathbf{A}_L^{-g} = \left(\mathbf{A}_L^{\mathrm{t}}\mathbf{C}_d^{-1}\mathbf{A}_L + \mathbf{C}_{m,L}^{-1}\right)^{-1}\mathbf{A}_L^{\mathrm{t}}\mathbf{C}_d^{-1}. \tag{8}$$

The forward matrix $\mathbf{A}_L$ is constructed for model parameters up to the (arbitrary) truncation level L, and the covariance matrix for the truncated model vector and data is denoted by $\mathbf{C}_{m,L}$ and $\mathbf{C}_d$, respectively, (Tarantola 1987; Menke 1989).

Rewriting $\mathbf{m}$ as a sum of $\mathbf{m}_L$ and $\mathbf{m}_\infty$ in eq. (6) shows the explicit dependence of the data upon partitioning:

$$\mathbf{d} = \mathbf{A}_L\mathbf{m}_L + \mathbf{A}_\infty\mathbf{m}_\infty + \mathbf{e}, \tag{9}$$

where $\mathbf{A}_\infty$ is the forward matrix corresponding to the infinitely dimensional model vector $\mathbf{m}_\infty$. Inserting eq. (9) into the least-squares solution for $\tilde{\mathbf{m}}_L$ in eq. (7) illustrates the effect of spectral leakage, and the estimated model vector $\tilde{\mathbf{m}}_L$ up to truncation level L is written as

$$\tilde{\mathbf{m}}_L = \mathbf{m}_L + \left(\mathbf{A}_L^{-g}\mathbf{A}_L - \mathbf{I}\right)\mathbf{m}_L + \mathbf{A}_L^{-g}\mathbf{A}_\infty\mathbf{m}_\infty + \mathbf{A}_L^{-g}\mathbf{e}. \tag{10}$$

The last three terms in eq. (10) are responsible for deviations from the true model $\mathbf{m}_L$. The second and the fourth term account for limitations in resolution in the L-dimensional subspace and the effects of data errors, respectively. The third term is due to spectral leakage and $\mathbf{A}_L^{-g}\mathbf{A}_\infty\mathbf{m}_\infty$ is the projection of the contribution of $\mathbf{m}_\infty$ in the data on to the truncated model vector $\tilde{\mathbf{m}}_L$.

The cure for spectral leakage in the least-squares sense is given in Trampert & Snieder (1996). To avoid notational complications, we assume the simplest case where the data covariance matrix is written as $\mathbf{C}_d = \sigma_d^2\mathbf{I}$ and the model covariances similarly as $\mathbf{C}_{m,L} = \sigma_{m,L}^2\mathbf{I}$ and $\mathbf{C}_{m,\infty} = \sigma_{m,\infty}^2\mathbf{I}$. Defining $\alpha^2 = \sigma_{\mathrm{d}}^2/\sigma_{m,L}^2$ and $\beta^2 = \sigma_{\mathrm{d}}^2/\sigma_{m,\infty}^2$, the least-squares solution for $\mathbf{m}_L$ corrected for spectral leakage is found to be

$$\tilde{\mathbf{m}}_L^W = \left[\mathbf{A}_L^{\mathrm{t}}\mathbf{W}\mathbf{A}_L + \left(\frac{\alpha^2}{\beta^2}\right)\mathbf{I}\right]^{-1}\mathbf{A}_L^{\mathrm{t}}\mathbf{W}\mathbf{d}, \tag{11}$$

with

$$\mathbf{W} = \left(\mathbf{A}_\infty\mathbf{A}_\infty^{\mathrm{t}} + \beta^2\mathbf{I}\right)^{-1}. \tag{12}$$

Unfortunately, the matrix $\mathbf{A}_\infty\mathbf{A}_\infty^{\mathrm{t}}$, which suppresses spectral leakage, is not necessarily invertible and a damping needs to be applied. In the Bayesian framework, as used here, β^2 expresses the relative importance of data errors versus the expected (or assumed) variance of the neglected model parameters.

By inspection, it is seen that the solution in eq. (11) corrected for spectral leakage has the same form as the simple least-squares solution in eq. (7), but of course the inverse operators differ. The ordinary least-squares solution is a special case of eq. (11) where β tends towards infinity. This is understandable since a high value of β means that less power is implicitly allowed to be explained by neglected basis functions (small $\sigma_{m,\infty}^2$). Eq. (10) is general and thus holds for both the classical least-squares inversion and the spectral leakage inversion. However, because of different inverse operators, the dependence of $\tilde{\mathbf{m}}_L$ upon the true model and the data errors is different in the two kinds of inversion approaches. Furthermore, the solution corrected for spectral leakage does not depend on $\mathbf{m}_\infty$ by construction. We will discuss the effects of limited resolution and error propagation on the solution below. In addition, it is useful to estimate the range of values for all parameters involved in a realistic global surface wave tomography experiment where real data can be quite noisy.

3 CORRECTING FOR SPECTRAL LEAKAGE

The problem in calculating $\mathbf{W}$ is to evaluate the matrix product $\mathbf{A}_\infty\mathbf{A}_\infty^{\mathrm{t}}$, which involves an infinite-dimensional calculation. The bias matrix in Trampert & Snieder (1996) shows that spectral leakage is highest for degrees closest to the truncation level. This suggests an approximate way to calculate the matrix product by including the next N degrees from the desired truncation level L resulting in an upper limit $l_{\max} = L + N$ needed for the calculation. This has been used in the synthetic experiment of Trampert & Snieder (1996). For real data, however, it is not obvious what the choice of N should be given a fixed L. A closed form of $\mathbf{A}_\infty\mathbf{A}_\infty^{\mathrm{t}}$ can be derived which involves the Gram matrix. For ray theoretical calculations, the data kernel is non-square-integrable and hence the Gram matrix is not defined. This problem is well known and there are several ways around it. The most common are integral quelling (Chou & Booker 1979), *a priori* model covariance functions (Tarantola & Nercessian 1984) and finite ray widths (Michelena & Harris 1991). We will use the latter technique where our ray widths are a direct consequence of including finite-frequency effects into the wave propagation problem. First-order scattering theory produces square-integrable data kernels. This allows us then to calculate $\mathbf{W}$ exactly and evaluate the effect of introducing an upper limit $l_{\max}$.

According to Spetzler *et al.* (2002), the relative phaseshift $d_{\rm scat}$ between a station and receiver can be written as a sum of spherical harmonics coefficients C_l^m multiplied by the Fréchet kernel $K_{l,m}^{\rm scat}$ for degree l and order m using first-order diffraction theory:

$$d_{\rm scat} = \sum_{l=0}^{\infty} \sum_{m=-l}^{l} C_l^m K_{l,m}^{\rm scat}. \tag{13}$$

The theory takes the finite period of surface waves into account, and it is valid for unconverted surface waves. The Fréchet kernel $K_{l,m}^{\rm scat}$ for degree l and order m is the projection of the sensitivity function $K^{\rm scat}(R, \theta, \varphi)$ on to the spherical harmonic $Y_l^m(\theta, \varphi)$ defined over the sphere Ω:

$$K_{l,m}^{\rm scat} = \int_{\Omega} K^{\rm scat}(R, \theta, \varphi) Y_l^m(\theta, \varphi)\, d\theta\, d\varphi. \tag{14}$$

The reader is referred to fig. 1 in Spetzler *et al.* (2002) for an example of the sensitivity function $K^{\rm scat}(R, \theta, \varphi)$. Comparing expression (5) with the Fréchet kernel in eq. (14), we see that the data kernel $G_i(x)$ corresponds to $K^{\rm scat}(R, \theta, \varphi)$ and the basis functions $B_j(x)$ to the spherical harmonics $Y_l^m(\theta, \varphi)$. In closed form, the matrix product $\mathbf{A}_\infty \mathbf{A}_\infty^{\rm t}$ in eq. (12) is then given by

$$\left\{\mathbf{A}_\infty \mathbf{A}_\infty^{\rm t}\right\}_{ij} = \int_{\Omega} K_i^{\rm scat}(R, \theta, \varphi) K_j^{\rm scat}(R, \theta, \varphi)\, d\theta\, d\varphi - \left\{\mathbf{A}_L \mathbf{A}_L^{\rm t}\right\}_{ij}, \tag{15}$$

where the subindexes in the sensitivity functions indicate the source–receiver pairs i and j. The integral in eq. (15) is well defined because the data kernels are square-integrable.

The calculation of $\mathbf{A}_\infty \mathbf{A}_\infty^{\rm t}$ with eq. (15) is very time consuming and thus impractical for a full tomographic inversion, but it allows one to evaluate the implications of approximating the matrix product by

$$\left\{\mathbf{A}_\infty \mathbf{A}_\infty^{\rm t}\right\}_{ij} = \sum_{s=L+1}^{l_{\rm max}} \{\mathbf{A}_\infty\}_{is} \left\{\mathbf{A}_\infty^{\rm t}\right\}_{sj}, \tag{16}$$

up to a suitable maximum angular degree $l_{\rm max}$ of the spherical harmonics expansion much higher than the truncation level L.

4 SYNTHETIC MODELLING EXPERIMENTS

To isolate the contribution of each of the terms in eq. (10) we performed several synthetic modelling experiments with a well-known input model. We show comparisons between inversions with spectral leakage corrections (eq. 11) and without (eq. 7).

In the synthetic modelling experiment, we used source–receiver positions from a subset of 10 000 Love wave phase velocity measurements from the data set of Trampert & Woodhouse (2001). The use of a subset is purely motivated by computer time requirements and in the subsequent real data example we used the complete surface wave data set. Fig. 1 shows the ray density obtained by the selected 10 000 measurements for the synthetic tests. The ray density is shown on a logarithmic scale and clearly presents a heterogeneous coverage. The highest ray density is on the Pacific Plate, in Eurasia and in North America while the poorest sampling is found on the Southern Hemisphere. The gradients in ray path coverage in the complete surface wave data set are similar to that in the selected 10 000 measurements.

The first term of eq. (10) is due to imperfect resolution and can be written as $(\mathbf{R} - \mathbf{I})\mathbf{m}_L$ where the resolution matrix $\mathbf{R} = \mathbf{A}_L^{-g}\mathbf{A}_L$. A comparison between a classical least-squares inversion and a spectral leakage corrected inversion can only be objective in the case of the same resolution matrix. It is difficult to obtain the same resolution as the two inverse operators are different, unless $\alpha = 0$ and then by definition $\mathbf{R} = \mathbf{I}$. This corresponds to the case of no overall damping and requires the inverse problem to be stable. Given our data coverage, an undamped expansion up to degree $L = 10$ is completely stable. This is probably a very conservative limit since with a similar data coverage, Ekström *et al.* (1997) made an undamped expansion to degree 16. The second term is $\mathbf{A}_L^{-g}\mathbf{A}_\infty \mathbf{m}_\infty$ and is due to spectral leakage itself. For clarity, we neglect data errors at the moment, but will treat the last term of eq. (10) later in this section. The resolution matrix being equal to the identity matrix, in the case of a spectral leakage corrected inversion eq. (10) reads

$$\tilde{\mathbf{m}}_L \approx \mathbf{m}_L. \tag{17}$$

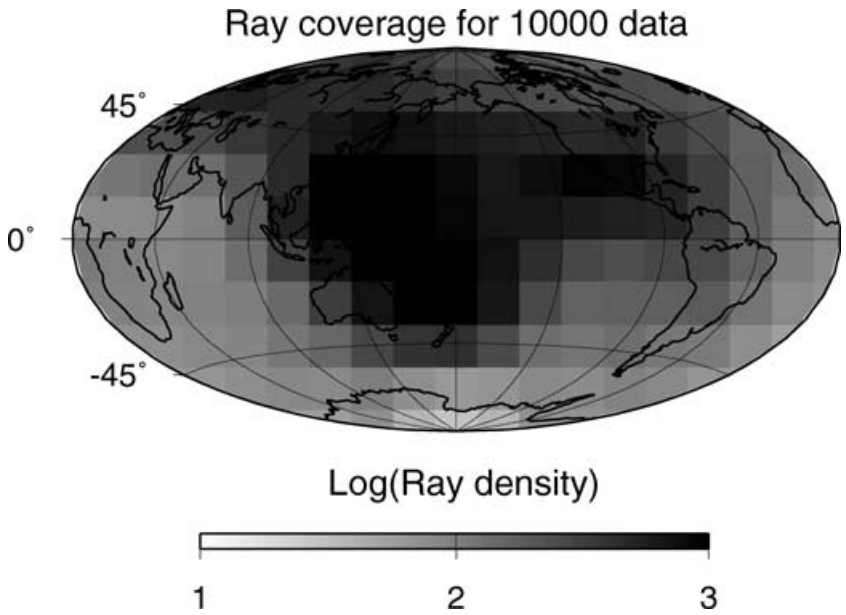

Figure 1. The ray coverage of 10 000 paths used in our synthetic modelling experiment The grey-scale shows the ray density on a base 10 logarithmic scale.

The last relation is only approximately true because the spectral leakage term is suppressed in the least-squares sense, but not exactly. On the other hand, in the case of an undamped ordinary least-squares inversion the estimated model is given by

$$\tilde{\mathbf{m}}_L = \mathbf{m}_L + \mathbf{A}_L^{-g}\mathbf{A}_\infty \mathbf{m}_\infty, \tag{18}$$

which differs from eq. (17) by the spectral leakage term $\mathbf{A}_L^{-g}\mathbf{A}_\infty\mathbf{m}_\infty$ only.

The synthetic experiment uses an input model built from two spherical harmonic components of degree 8 and 12 only. The objective is to recover a model truncated at degree $L = 10$. The synthetic input model has a long- and a short-wavelength structure, and if no spectral leakage occurs, we should only recover the degree 8 part. The amplitude of relative phase velocity perturbation is 5 per cent for both, the large- and the small-scale structure. Synthetic average relative phaseshifts for 150 s fundamental mode Love waves are computed using surface wave scattering theory (eq. 13) and the 10 000 source–receiver positions from Fig. 1. The synthetic data are noise-free.

The antileakage matrix $\mathbf{W}$ in eq. (12) depends on two additional parameters, β and the maximum angular order $l_{\max}$ used to approximate $\mathbf{A}_\infty\mathbf{A}_\infty^{\mathrm{t}}$ in eq. (16). To check the accuracy of this approximation, we use the closed form in eq. (15). It turns out that the off-diagonal elements using eq. (16) converge quickly to those using eq. (15). The diagonal elements converge very slowly. This is fortunate because the diagonal elements trade-off with the value of β. We find that as long as $l_{\max}$ is at least twice as large as L, the approximation from eq. (16) is sufficient. β is then used to adjust the diagonal elements in order to stabilize the inverse of $\mathbf{A}_\infty\mathbf{A}_\infty^{\mathrm{t}}$. The optimal value of β is given by the peak of the histogram of the diagonal values of $\mathbf{A}_\infty\mathbf{A}_\infty^{\mathrm{t}}$ obtained from eq. (16). Choosing a value higher than the peak quickly diminishes the effect of leakage correction and the higher β, the closer the result is to the ordinary least-squares solution. Choosing a value smaller than the peak, does not change the results significantly provided the inverse of $\mathbf{A}_\infty\mathbf{A}_\infty^{\mathrm{t}}$ remains stable.

The results are illustrated by looking at the amplitude spectra of the different solutions. We define the rms amplitude of a model at angular degree l as

$$\mathrm{rms}(l) = \sqrt{\frac{\sum_{m=-l}^{l}\left(a_l^m\right)^2}{4\pi}}, \tag{19}$$

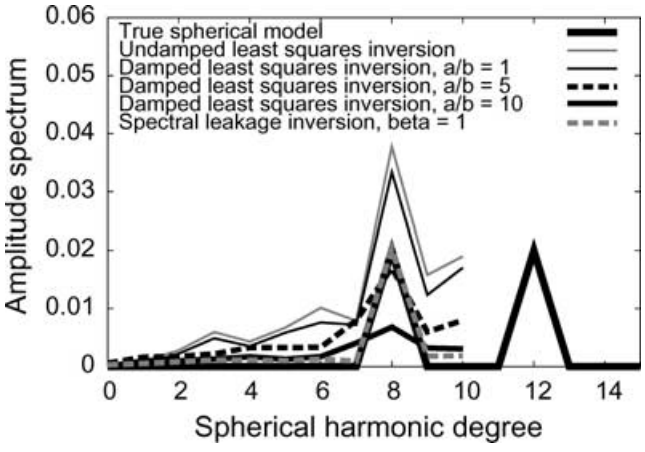

Figure 2. Amplitude spectra of the input model and several inverted models.

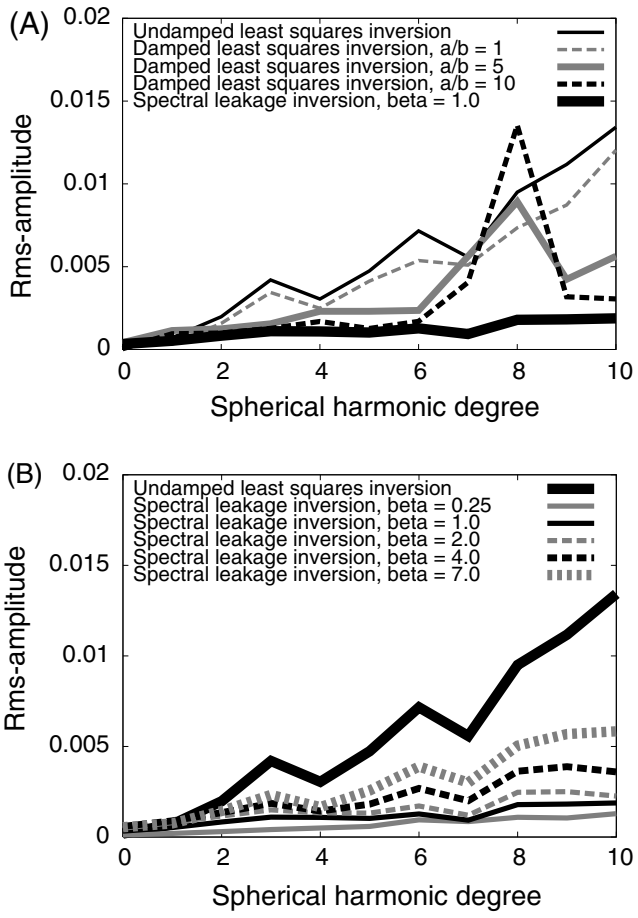

Figure 3. Amplitude spectra of the difference between the true and estimated models: (a) for several least-squares inversions and a spectral leakage corrected inversion; (b) several spectral leakage solutions for different values of β.

where a_l^m is the spherical harmonic coefficient of the model at angular degree l and order m. In Fig. 2, the amplitude spectra of different least-squares inversion and the spectral leakage solution with optimal β are shown. The input model is plotted as a reference. It is clear that the undamped least-squares inversion has significant unwanted power at degrees 9 and 10. Damping can reduce this power,

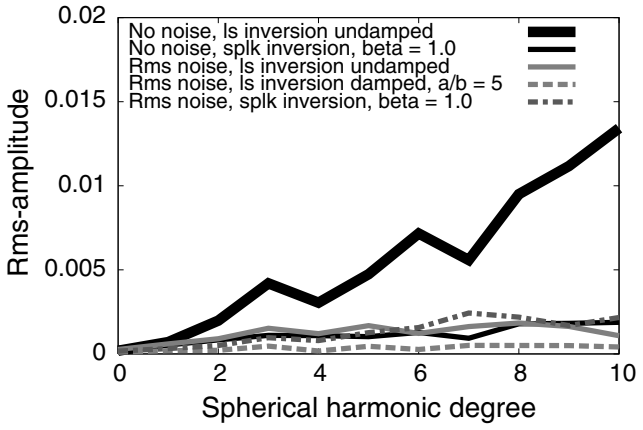

Figure 4. Amplitude spectra of the difference between the true and inverted models from the least-squares (ls) inversion and spectral leakage (splk) inversion in the synthetic experiment, wherein the noise term is compared with the spectral leakage term. $\beta = 1.0$ in the spectral leakage experiment.

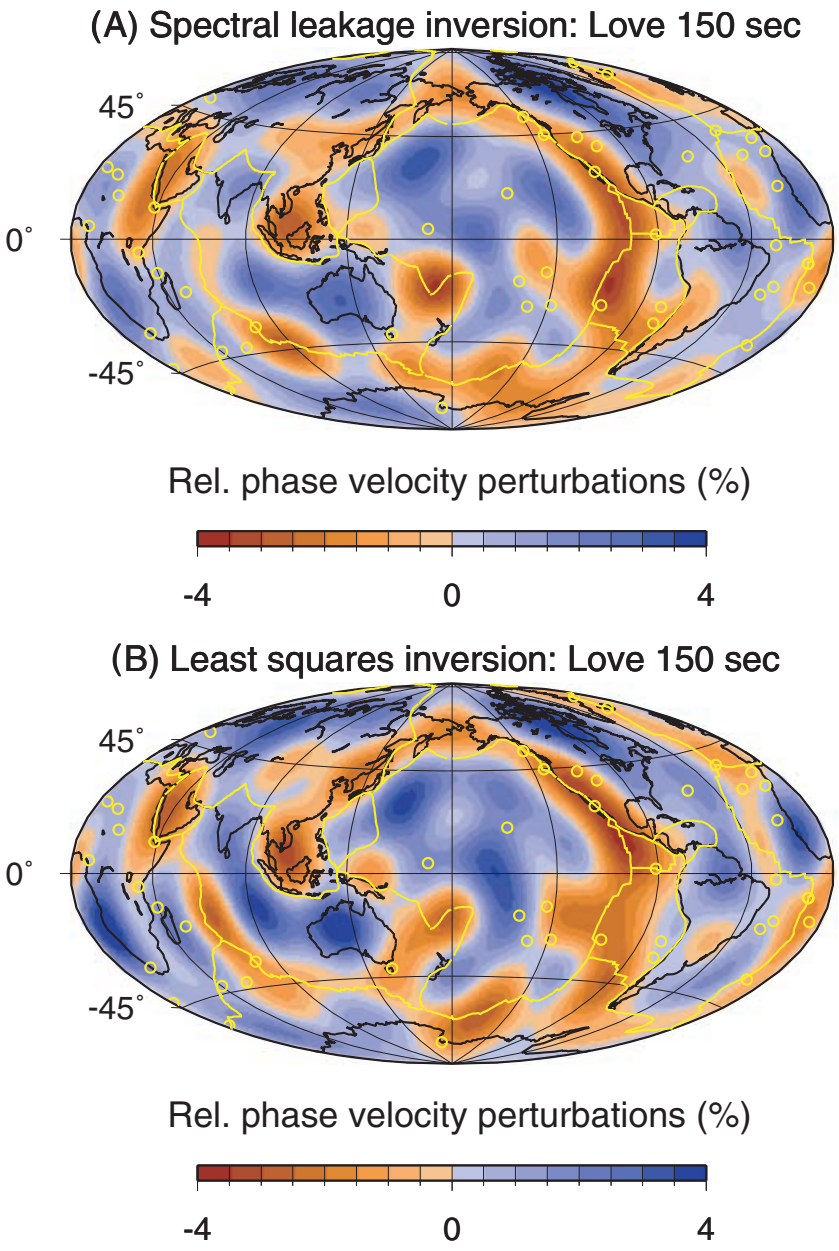

Figure 5. Global phase velocity models for Love waves at 150 s from a spectral leakage inversion and an undamped least-squares inversion. The yellow circles are hotspots, the yellow lines show the boundaries between tectonic plates and coastlines are drawn with the black lines. The variations in the relative phase velocity perturbations are given in per cent on a scale ±4 per cent with respect to the PREM model. The models are expanded to degree 10 in spherical harmonics. (a) The phase velocity map obtained including spectral leakage corrections. The parameters are $\alpha = 0$ and $\beta = 0.5$. (b) The phase velocity map obtained from a least-squares inversion without any damping.

but will seriously distort degree 8 as well. Only the spectral leakage corrected inversion is close to the input model at all degrees. The different behaviour of (damped) least-squares inversion and spectral leakage corrected inversions are perhaps best seen on plots of amplitude spectra of the difference between input and output models (Fig. 3a). The undamped least-squares inversion has an increasing difference power up to the truncation level. Increasing damping reduces that slope, but an unwanted peak appears at degree 8. We also show the effect of β on the effectiveness of spectral leakage reduction and how increasing β converges towards the least-squares solution (Fig. 3b).

The last term of eq. (10) is the contribution from data errors. The inverse operators $\mathbf{A}_L^{-g}$ differ, depending on whether the spectral leakage corrections are included or not, and hence the effect of data errors contaminating the estimated models manifests itself differently in the two cases. Again a synthetic modelling experiment is used to estimated the importance of the term $\mathbf{A}_L^{-g}\mathbf{e}$. We assume that the noise has similar statistics for each measurement and is uncorrelated. Let σ_d denote the standard deviation of this noise so that $\mathbf{e} = \sigma_\mathrm{d}\mathbf{l}$. The relative rms error of the 150 s Love wave measurements of Trampert & Woodhouse (2001) is 40 per cent. We adopt this value here and σ_d is given by

$$\sigma_\mathrm{d} = 0.4\sqrt{\frac{\sum_{i=1}^{n_\mathrm{data}} d_i^2}{n_\mathrm{data}}}, \tag{20}$$

where d_i is a data point calculated from our synthetic input model of degree 8 and 12 only, and $n_{\text{data}} = 10\,000$ is the number of data points in the experiment. Fig. 4 shows the amplitude spectra of the term $\mathbf{A}_L^{-g}\mathbf{e}$ for the simple least squares approach and the spectral leakage inversion compared with the term $\mathbf{A}_L^{-g}\mathbf{A}_\infty\mathbf{m}_\infty$ for several cases. Overall, data errors affect the solution less than neglecting spectral leakage. We further noticed a trade-off between spectral leakage reduction and noise suppression which is controlled by β. Spectral leakage reduction requires the smallest possible value for β (which cannot be zero for stability reasons), while error reduction requires the highest possible value. The best compromise is found if β corresponds to the peak of the histogram of the diagonal elements of $\mathbf{A}_\infty\mathbf{A}_\infty^{\text{t}}$. This trade-off does not come as a surprise. Spectral leakage reduction is optimized for small β. Increasing β makes the solution converge towards the least-squares solution which is optimized for error reduction.

5 PHASE VELOCITY MAPS

We use the full data set (41 016 measurements) of Trampert & Woodhouse (2001) to calculate phase velocity maps for 150 s Love waves using the classical least-squares inversion and spectral leakage corrections, respectively. The truncation level is $L = 10$ so that we do not need any overall damping and the comparisons are not blurred by a limited resolution. The inversion of this large data set with spectral leakage corrections has been carried out on a 64-bit shared memory computer (see acknowledgments). The relative phase velocity map for 150 s Love waves using the spectral leakage corrections is shown in Fig. 5(a), while the ordinary least-squares solution is plotted in Fig. 5(b). Comparing the estimated phase velocity models, we see a good agreement between both phase velocity maps in the long-wavelength structure. However, in the shorter-wavelength structure close to the truncation level there are significant differences for several tectonic features. This prominent difference for degrees closest to 10 is best seen in the correlation between the two models (Fig. 6). The plate boundaries most affected by spectral leakage are the Carlsberg ridge, the South-West Indian ridge, the East Pacific rise, the Peru-Chili trench, the Mid-Atlantic ridge and the Japan trench. Since we do not know the true Earth, we cannot easily decide which is the best model. The synthetic tests, however, strongly suggest that the spectral leakage corrected model is closer to the true Earth. Sometimes undamped low-degree least-squares inversions are used to reject outliers in data sets (e.g. Ekström *et al.* 1997). Our example shows that because of spectral leakage, measurements could be incorrectly declared outliers in many places on the globe.

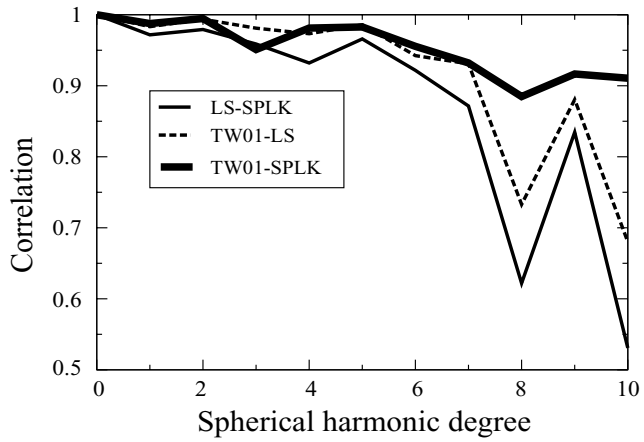

Figure 6. Correlation as a function of spherical harmonic degree between the 150 s Love wave model (TW01) of Trampert & Woodhouse (2001) and our ordinary least-squares model (LS) from Fig. 5(b) (thin dotted line) and our model including spectral leakage correction (SPLK) from Fig. 5(a) (thick solid line). Also shown is the correlation between our models (LS and SPLK) from Figs 5(a) and (b) (thin solid line). All correlation are above the 99 per cent confidence level.

6 DISCUSSION AND CONCLUSION

It is clear from the synthetic modelling experiments of global surface wave data that spectral leakage may bias models if no special precaution is taken. Ordinary damping cannot correct for spectral leakage and its effect is bigger than that induced by data errors and thus should to be taken seriously.

The theory to compensate for the spectral leakage effect is based on a specific weighting in the data space which is its main drawback. Inverting a matrix of the size of the number of data is very computer intensive. Knowing that the main degrees affected by spectral leakage are those close to the truncation level, suggests an alternative. If the desired truncation level is again L, the model should be expanded to $L + N$ where N could be much larger than L before the difficulty of a data size matrix would be reached. Inverting for more parameters increases the instability of the inverse problem and damping is certainly required. The nature of the problem is such that the highest degrees need the most damping. If model size damping is chosen, damping is uniform for all degrees and the highest degrees will impose a damping which will clearly involve the lowest degrees. We prefer Laplacian damping, which imposes increased damping with increasing degree, thus effectively controlling the highest degrees without affecting the lower ones too much. This is shown qualitatively in Fig. 6 where the correlation between the spectral leakage corrected model and the Laplacian damped degree 40 model of Trampert & Woodhouse (2001) is illustrated. The overall high correlation indicates that overparametrization ensures that the lowest degrees remain unaffected by spectral leakage. The drawback of this approach is that the resulting varying lateral and vertical resolution make geodynamic interpretations not straightforward. The aim is to produce more accurate Earth models showing smaller and smaller scale structure. To make useful interpretations of such models (e.g. the decay of power spectra, the depth extent of features) we will have to move away from damped inversions and explicitly avoid spectral leakage.

The spectral leakage corrections to the complete surface wave data set of Trampert & Woodhouse (2001) took 10 CPU-days on a fast shared memory computer (500 MHz clock frequency). The synthetic modelling experiment, using 10 000 data points only (four times less than the real data) was performed on a single-processor Pentium IV Linux system with 1 Gb internal memory and the CPU time was 6 h. Although computer intensive, spectral leakage corrections will become increasingly feasible with the availability of faster computer systems with large shared memory facilities.

ACKNOWLEDGMENTS

This work was partly supported by the Dutch National Science Foundation under contract number NWO-GOA-750.297.02. In addition, we are grateful to NCF (Nederlandse Computer Faciliteiten) for financial support to use their computer system *SARA* in Amsterdam. Without *SARA*, we could not have applied spectral leakage

corrections using the complete surface wave data set. We thank the two anonymous reviewers for constructive comments.

REFERENCES

Chou, C.W. & Booker, J.R., 1979. A Backus–Gilbert approach to inversion of traveltime data for three-dimensional velocity structure, *Geophys. J. R. astr. Soc.,* **59,** 325–344.

Ekström, G., Tromp, J. & Larson, E.W.F., 1997. Measurements and global models of surface wave propagation, *J. geophys. Res.,* **59,** 8137–8157.

Menke, W., 1989. *Geophysical Data Analysis: Discrete Inverse Theory,* Academic, New York.

Michelena, R.J. & Harris, J.M., 1991. Tomographic traveltime inversion using natural pixels, *Geophysics,* **59,** 635–644.

Snieder, R. & Trampert, J., 1999. Inverse problems in geophysics, in, Wavefield *Inversion,* ed. Wirgin, A., Springer, New York.

Snieder, R., Beckers, J. & Neele, F., 1991. The effect of small-scale structure on normal mode frequencies and global inversions, *J. geophys. Res.,* **59,** 501–515.

Spetzler, J., Trampert, J. & Snieder, R., 2002. The effect of scattering in surface wave tomography, *Geophys. J. Int.,* **149,** 755–767.

Tarantola, A., 1987. *Inverse Problem Theory: Methods for Data Fitting and Model Parameter Estimation,* Elsevier, New York.

Tarantola, A. & Nercessian, A., 1984. Three-dimensional inversion without blocks, *Geophys. J. R. astr. Soc.,* **59,** 299–306.

Trampert, J. & Snieder, R., 1996. Model estimations biased by truncated expansions: possible artifacts in seismic tomography, *Science,* **271**, 1257–1260.

Trampert, J. & Woodhouse, J.H., 2001. Assessment of global phase velocity models, *Geophys. J. Int.,* **144,** 165–174.

Wang, Z. & Dahlen, F.A., 1995. Validity of surface-wave ray theory on a laterally heterogeneous Earth, *Geophys. J. Int.,* **123,** 757–773.